Fungal dual-domain LysM effectors undergo chitin-induced intermolecular, and not intramolecular, dimerization

Hui Tian[1,2], Gabriel L. Fiorin[2], Anja Kombrink[2], Jeroen R. Mesters[3,#], Bart P.H.J. Thomma[1,4,#,*]

[1]University of Cologne, Institute for Plant Sciences, 50674 Cologne, Germany; [2]Laboratory of Phytopathology, Wageningen University and Research, Droevendaalsesteeg 1, 6708PB Wageningen, The Netherlands; [3]Institute of Biochemistry, University of Lübeck, Ratzeburger Allee 160, 23538 Lübeck, Germany; [4]University of Cologne, Institute for Plant Sciences, Cluster of Excellence on Plant Sciences (CEPLAS), 50674 Cologne, Germany.

[#]These authors contributed equally

*To whom correspondence should be addressed. E-mail: bthomma@uni-koeln.de

Running head: Dual-domain LysM effectors undergo polymerization.

SUMMARY

Chitin is a homopolymer of β-(1,4)-linked *N*-acetyl-D-glucosamine (GlcNAc) and a major structural component of fungal cell walls. In plants, chitin acts as a microbe-associated molecular pattern (MAMP) that is recognized by lysin motif (LysM)-containing plant cell surface-localized pattern recognition receptors (PRRs) that activate a plethora of downstream immune responses. In order to deregulate chitin-induced plant immunity and successfully establish infection, many fungal pathogens secrete LysM domain-containing effector proteins during host colonization. It was previously shown that the LysM effector Ecp6 from the tomato leaf mould fungus *Cladosporium fulvum* can outcompete plant PRRs for chitin binding because two of its three LysM domains cooperate to form a composite groove with ultra-high (pM) chitin-binding affinity. However, most functionally characterized LysM effectors contain only two LysMs, including *Magnaporthe oryzae* MoSlp1, *Verticillium dahliae* Vd2LysM, and *Colletotrichum higginsianum* ChElp1 and ChElp2. Here, we performed modelling, structural and functional analyses to investigate whether such dual-domain LysM effectors can also form ultra-high chitin-binding affinity grooves through intramolecular LysM dimerization. However, our study suggests that intramolecular LysM dimerization does not occur. Rather, our data support the occurrence of intermolecular LysM dimerization for these effectors, associated with a significantly lower chitin binding affinity than monitored for Ecp6. Interestingly, the intermolecular LysM dimerization allows for the formation of polymeric complexes in the presence of chitin. Possibly, such polymers may precipitate at infection sites in order to eliminate chitin oligomers, and thus suppress the activation of chitin-induced plant immunity.

41 **INTRODUCTION**

42 Chitin is a homopolymer of β-(1,4)-linked *N*-acetyl-D-glucosamine (GlcNAc) and a major
43 structural component of fungal cell walls (Lenardon et al., 2010; Free, 2013). In plants,
44 chitin has been characterized as a fungal microbe-associated molecular pattern (MAMP)
45 that can be recognized by cell surface-localized pattern recognition receptors that
46 contain extracellular lysin motif (LysM) domains (LysM-PRRs) (Zhang et al., 2007; Zipfel,
47 2008; Sanchez-Vallet et al., 2015; Rovenich et al., 2016). Upon recognition of chitin by
48 such receptors, plants evoke a broad range of immune responses, including the
49 generation of ion fluxes, the production of reactive oxygen species (ROS), the activation
50 of mitogen-associated protein kinases (MAPKs) and the expression of defence-related
51 genes that include those encoding hydrolytic enzymes, such as chitinases, in order to
52 halt fungal invasion (Felix et al., 1993; Jones and Dangl, 2006; Altenbach and Robatzek,
53 2007; Boller and Felix, 2009; Sanchez-Vallet et al., 2015). LysM-PRRs have been
54 functionally characterized in several plants, including the model plant Arabidopsis
55 (*Arabidopsis thaliana*) in which the LysM receptor AtLYK5 was reported to bind chitin
56 with high affinity (1.72 μM) and form a tripartite receptor complex with AtLYK4 and
57 AtCERK1 to initiate chitin signalling (Cao et al., 2014). AtCERK1 was found to bind chitin
58 directly as well, albeit with significantly lower affinity than AtLYK5 (Miya et al., 2007;
59 Petutschnig et al., 2010; Cao et al., 2014).

60 To overcome chitin-induced immunity, successful fungal pathogens evolved
61 various strategies to either protect fungal cell wall chitin against hydrolysis by host
62 enzymes, or prevent the activation of plant immunity by fungal cell wall-derived chitin
63 oligomers (de Jonge et al., 2010; Rovenich et al., 2014; Sanchez-Vallet et al., 2015). For
64 the fungus *Cladosporium fulvum*, causal agent of leaf mould disease of tomato, several
65 strategies to deal with chitin-triggered immunity have been characterized. During host

66 colonization, *C. fulvum* secretes the effector protein Ecp6 that contains three LysMs and
67 binds chitin oligosaccharides with ultra-high affinity, leading to the suppression of
68 chitin-induced plant immune responses (Bolton et al., 2008; de Jonge et al., 2010). A
69 crystal structure of Ecp6 revealed that two of its three LysMs cooperate to form a
70 composite chitin-binding groove that binds chitin through intrachain LysM dimerization
71 (Sanchez-Vallet et al., 2013). *Zymoseptoria tritici*, the causal agent of Septoria tritici
72 blotch (STB) of wheat, secretes the LysM effector Mg3LysM, a close homolog of Ecp6,
73 that similarly suppresses chitin-triggered immunity (Marshall et al., 2011). Additionally,
74 *Z. tritici* secretes two effectors that comprise a single LysM only, Mg1LysM and
75 Mgx1LysM that were both characterized to protect hyphae against hydrolysis by plant
76 chitinases and to suppress chitin-triggered immunity in plants (Marshall et al., 2011;
77 Tian et al., 2021). An Mg1LysM crystal structure showed that two Mg1LysM monomers
78 form a chitin-independent homodimer via the β-sheet in the *N*-terminus of Mg1LysM
79 (Sánchez-Vallet et al., 2019). Furthermore, Mg1LysM homodimers were shown to
80 undergo ligand-induced polymerization in the presence of chitin, leading to a polymeric
81 structure that is able to protect fungal cell walls (Sánchez-Vallet et al., 2019). Similar
82 chitin-induced homopolymer formation was shown for Mgx1LysM (Tian et al., 2021).

83 Suppression of chitin-triggered immunity by secreted fungal effectors that carry
84 no other recognizable domains than LysM domains, collectively referred to as LysM
85 effectors, has been demonstrated for various phytopathogenic fungi. For instance,
86 *Magnaporthe oryzae*, the causal agent of rice blast disease, secretes the LysM effector
87 Slp1 to bind chitin and suppress chitin-triggered immune responses (Mentlak et al.,
88 2012). Similarly, the Brassicaceae anthracnose fungus *Colletotrichum higginsianum*
89 secretes ChElp1 and ChElp2, while the broad host-range vascular wilt fungus
90 *Verticillium dahliae* secretes Vd2LysM (Takahara et al., 2016; Kombrink et al., 2017).

While these examples are from plant-associated Ascomycete fungi, also plant-associated fungi that belong to other phyla utilize LysM effectors to suppress chitin-triggered immunity. For instance, the Basidiomycota soil-borne broad host-range pathogen *Rhizoctonia solani* secretes RsLysM, while the Glomeromycota arbuscular mycorrhizal fungus *Rhizophagus irregularis* secretes RiSLM to suppress chitin-triggered immunity (Dolfors et al., 2019; Zeng et al., 2020). The latter example demonstrates that also non-pathogenic fungi utilize LysM effectors in their interactions with host plants. Moreover, the finding that LysM effectors contribute to the virulence of the Ascomycete fungus *Beauveria bassiana* by evasion of immune responses in insect hosts demonstrates that LysM effectors play roles in fungal interactions beyond plant hosts (Kombrink and Thomma, 2013; Cen et al., 2017).

Based on the functional analysis of *C. fulvum* Ecp6, it has been proposed that the ability to suppress chitin-triggered immunity resides in the ability to form a composite chitin-binding groove through intrachain LysM dimerization to bind chitin with ultrahigh affinity, such that host chitin receptors are outcompeted for substrate binding (Sanchez-Vallet et al., 2013; Sanchez-Vallet et al., 2015). However, most LysM effectors that are functionally characterized today contain only two LysMs; so-called dual-domain LysM effectors. It has remained unclear thus far whether these dual-domain LysM effectors are able to undergo intramolecular LysM dimerization, like in Ecp6, to establish ultrahigh affinity chitin-binding sites, or whether chitin binding by these effectors is based on another mechanism.

113 **RESULTS**

114 **Structural prediction precludes intrachain LysM dimerization**

115 It has previously been determined that *M. oryzae* MoSlp1, *V. dahliae* Vd2LysM, and *C.*
116 *higginsianum* ChElp1 and ChElp2 comprise two LysM domains, bind chitin and suppress
117 chitin-induced host immunity (Mentlak et al., 2012; Takahara et al., 2016; Kombrink et
118 al., 2017). Their length ranges from 145 aa (for Vd2LysM) to 176 aa (for ChElp2), with
119 the molecular weight of the mature proteins ranging from 14.24 to 16.14 kDa (Fig. 1A).
120 An amino acid sequence alignment of their LysM domains with those of *C. fulvum* Ecp6
121 displayed significant conservation of the domains, and of the residues involved in chitin
122 binding in particular (Fig. 1B). LysM domains are compact modules that display a β-α-α-
123 β secondary structure motif (Bateman and Bycroft, 2000) in which the termini of the
124 beta sheets are typically kept together by a disulfide bond at the LysM domain borders.
125 In Ecp6, three disulfide bonds are found within the individual LysM domains (LysM1:
126 C7-C61; LysM2: C80-C134; LysM3: C139-C191) and a fourth bond (C35-C69) locates in
127 between LysM1 and the linker between the two LysMs (Fig. 1C). Accordingly, in MoSlp1,
128 Vd2LysM, ChElp1 and ChElp2 the cysteines to form a disulfide bond within each of the
129 individual LysM domains are conserved and, similar to Ecp6, those to generate another
130 disulfide bond in between LysM1 and the linker between the two LysM domains
131 (MoSlp1: C46-C80; Vd2LysM: C31-C69; ChElp1: C56-C90; ChElp2: C62-C96) are
132 conserved as well (Fig. 1C). Intriguingly, these latter disulfide bonds will anchor a
133 significant part of the linker between the two LysM domains to the beginning of the
134 second α-helix of LysM1 in each of these effectors, severely limiting the part of the linker
135 that remains free to rotate. This is the most extreme for Vd2LysM, for which ten of the
136 19 amino acids of the linker between the two LysMs become fixed and a flexible stretch
137 of only nine amino acids remains (Fig. 1C).

138 To assess whether intramolecular LysM dimerization can occur in the dual-
139 domain LysM effectors, all four proteins were modelled based on the LysM1-LysM3
140 composite chitin binding groove of Ecp6 using Phyre2, I-TASSER and AlphaFold (Roy et
141 al., 2010; Yang and Zhang, 2015; Kelley et al., 2015; Jumper et al., 2021). Phyre2
142 successfully superposed the LysM domains of each of the effectors on LysM1 and LysM3
143 of Ecp6. Moreover, the software successfully predicted the disulfide bond that anchors a
144 significant part of the linker between the two LysM domains to the beginning of the
145 second α-helix of LysM1 for all LysM effectors but Vd2LysM (Fig. 2). However, all four
146 structure predictions displayed a disruption of the linker between the LysM domains
147 (Fig. 2), suggesting that (the flexible part of) the linkers of MoSlp1, Vd2LysM, ChElp1 and
148 ChElp2 are too short to accommodate intramolecular LysM dimerization. Accordingly,
149 an artificial insertion of a 5-amino acid sequence (GGSGG) in the linker of ChElp2 led to
150 predicted intramolecular LysM dimerization in a structure model with an uninterrupted
151 loop and a root-mean-square deviation (r.m.s.d.) value of 0.16 Å for 499 atom pairs (Fig.
152 2).

153 The I-TASSER prediction did not result in the display of disrupted linkers.
154 However, whereas the modelling was attempted on the composite binding groove of
155 Ecp6 composed by LysM1 and LysM3, I-TASSER modelled the structure of the LysM
156 effectors on LysM2 and LysM3 of Ecp6 (Fig. 2), r.m.s.d. values ranging from 0.49 Å (442
157 atom pairs) for ChElp2, 0.60 Å (470 atom pairs) for ChElp21, 0.64 Å (508 atom pairs) for
158 MoSlp1 to 1.67 Å (395 atom pairs) for Vd2LysM. Thus, like Phyre2, also the I-TASSER
159 modeling suggests that intramolecular LysM dimerization is not likely.

160 Also the third prediction software, AlphaFold, yielded structure models that were
161 not compatible with intramolecular chitin binding, with r.m.s.d. values as high as 2.62 Å
162 (567 atom pairs) and 5.42 Å (602 atom pairs) for ChElp2 and MoSlp1, respectively (Fig.

163 2). The ChElp1 structure model appeared compatible with intramolecular chitin binding
164 displaying an overall r.m.s.d. value of 0.153 Å (541 atom pairs). However, the low r.m.s.d.
165 value was only attainable because none of the anticipated disulfide bonds (C28-C83,
166 C56-C90 and C99-C152) materialized in the model. Especially C99 appears completely
167 out of position because the last three C-terminal amino acids including C152 are lacking
168 in the model (Fig. 2). The overall lack of cystins in the model permitted the flexible loop
169 between the two LysM domains to take a shortcut route, thereby ending in a dubious
170 model abandoning the basic features of a LysM domain. Surprisingly, in the Vd2LysM
171 model a different cysteine pair occurred, C5-C59, C31-C101 and C69-C124, resulting in a
172 model in which the two chitin binding motifs are pointing in opposite directions. Taken
173 together, all predictions based on the various software packages do not support
174 intramolecular chitin binding.
175

176 **Crystallization attempts for the LysM effectors failed**

177 The most direct method to reveal the chitin-binding mechanism of a LysM effector is by
178 determination of a three-dimensional protein structure in the presence of chitin, for
179 instance by X-ray crystallography, as previously performed for the single-domain LysM
180 effector Mg1LysM (Sánchez-Vallet et al., 2020) and the three-domain LysM effector Ecp6
181 (Sánchez-Vallet et al., 2013). Thus, we pursued this strategy for the dual-domain LysM
182 effectors as well. This strategy requires a protein crystal of sufficient size and quality to
183 be used in an X-ray diffraction experiment, which in turn requires highly pure protein of
184 a sufficiently high concentration. To this end, the four dual-domain LysM effectors were
185 heterologously produced in the yeast *Pichia pastoris* (Fig. S1A). Whereas MoSlp1
186 possesses four potential glycosylation sites (**N**^{48}DT, **N**^{94}IS, **N**^{130}LS and **N**^{104}NT), ChElp1
187 and ChElp2 contain only a single potential glycosylation site (**N**^{105}TS and **N**^{111}TS) and

188 Vd2LysM is not predicted to possess any glycosylation site (Fig. 1C) which corresponds
189 to findings in a glycoprotein staining assay (Fig. S1B). Nevertheless, attempts to remove
190 potential glycan chains did not lead to decreased molecular sizes of MoSlp1, Vd2LysM
191 and ChElp2 while fetuin as positive control revealed a clear size shift already at 2 h after
192 incubation (Fig. S1C). As we have previously successfully crystallized Ecp6 protein that
193 was produced in the same manner despite containing two spatially close glycosylation
194 sites that were indeed found to be glycosylated in the crystal structure (Sanchez-Vallet
195 et al., 2013), we decided to continue with these protein preparations. Also, the molecular
196 homogeneity of the protein solutions was improved by gel filtration combined with the
197 treatment with the nonionic detergent decyl β-D-maltopyranoside (DM) (Fig. S2).
198 Subsequently, all four proteins were subjected to extensive crystallization screenings. In
199 addition, ChElp2 and Vd2LysM were produced in *Escherichia coli* and subjected to
200 crystallization screenings as well. Unfortunately, none of the conditions tested resulted
201 in a genuine protein crystal for any of the dual-domain LysM effectors. Although
202 crystallization is an empirical process and there are many reasons why no crystals are
203 obtained, we reasoned that the lack of intramolecular chitin binding may also hamper
204 crystal growth.
205

206 **Chitin-induced intermolecular dimerization leads to LysM effector polymerization**

207 As all our crystallization attempts for the four dual-domain LysM effectors failed, we
208 pursued other strategies to provide evidence for the mechanism of chitin binding. We
209 reasoned that treatment with chitin oligomers would lead to higher order oligomeric or
210 polymeric protein complexes if intermolecular LysM dimerization occurs (Fig. 3A,
211 hypothesis I), while such complexes will not be formed in case of intramolecular LysM
212 dimerization (Fig. 3A, hypothesis II). To address these alternative hypotheses, ChElp2

213 was selected as a representative and expressed in *E. coli* to obtain protein that is devoid
214 of chitin. ChElp2 was produced either with a His-sumo-tag (14 kDa) or with a FLAG-tag
215 (1 kDa) and both forms were incubated together in the absence and presence of chitin.
216 His-sumo-tagged ChElp2 was pulled-down with anti-His magnetic beads and the
217 subsequent western blot (WB) result showed that FLAG-tagged ChElp2 was associated
218 with His-sumo-tagged ChElp2 only in the presence of chitin (Fig. 3B), indicating chitin-
219 induced intermolecular interactions between ChElp2 monomers.

220 To provide further evidence for chitin-induced intermolecular interactions, we
221 assessed the ChElp2 particle size distribution in solution upon chitin addition with
222 dynamic light scattering (DLS). Chitin addition at a molar ratio of 1:3 (protein:chitin)
223 shifted a portion of ChElp2 particles from around 10 nm in the absence of chitin to 100
224 nm in the presence of chitin (Fig. 4A). Further increase of exogenously added chitin to a
225 molar ratio of 1:6 significantly reduced the signal at 10 nm while inducing a strong
226 signal at 10 μm (Fig. 4A), indicative of chitin-induced polymerization of ChElp2. To
227 demonstrate the requirement of chitin binding for the observed polymerization, we
228 produced a ChElp2 mutant in which the threonine within each of the LysM domains that
229 is critical for chitin binding (LysM1, T49; LysM2, T120) was replaced by tryptophan,
230 produced the mutant in *E. coli*, and confirmed the compromised chitin binding affinity
231 by isothermal titration calorimetry (ITC) (Fig. 4B). Subsequently, the ChElp2$^{T49W\text{-}T120W}$
232 mutant was subjected to DLS analysis in the presence of exogenously added chitin,
233 revealing that the particle size shift that is observed for wild-type ChElp2 was not
234 observed for the mutant (Fig. 4A). Thus, we conclude that chitin binding is required for
235 ChElp2 polymerization.

236 As an additional line of evidence, we hypothesized that if ChElp2 undergoes
237 chitin-induced polymerization, we should be able to precipitate polymeric complexes

238 during centrifugation. Thus, we incubated ChElp2, and ChElp2$^{T49W-T120W}$ and Ecp6 as
239 negative controls, overnight with chitohexaose and subsequently centrifuged the
240 samples at 20,000 g in the presence of 0.002% methylene blue to visualize the protein.
241 As expected, a clear protein pellet appeared when ChElp2 was incubated with chitin, but
242 not in the control treatment without chitin, nor in the ChElp2$^{T49W-T120W}$ and Ecp6
243 samples (Fig. 4C; Fig. 6). Thus, we confirmed that chitin binding is required for ChElp2
244 polymerization.

245 To provide further evidence that specific chitin binding, rather than presence of
246 chitin or other carbohydrates, is required for ChElp2 polymerization, 100 μM ChElp2
247 was incubated with 1 mM diacetyl-chitobiose (Chi2), triacetyl-chitotriose (Chi3),
248 tetraacetyl-chitotetraose (Chi4), pentaacetyl-chitopentaose (Chi5), hexaacetyl-
249 chitohexaose (Chi6) or glucose. After centrifugation, protein pellets were observed for
250 ChElp2 incubations with Chi3, Chi4, Chi5 and Chi6, but not with Chi2 or glucose (Fig. 5A).
251 Arguably, given their differences in length, equimolar amounts of the various chitin
252 oligomers result in different final amounts of GlcNAc units. Thus, we repeated the assay
253 upon calibrating the various chitin oligomers such that the final amount of GlcNAc units
254 is the same in the various incubations. Also under these conditions, no protein pellets
255 formed upon incubation with Chi2 (Fig. 5B). Considering that a LysM domain binds
256 chitin oligomers that are composed of minimum three GlcNAc units, our findings
257 support that chitin binding, rather than mere chitin addition, is required for pellet
258 formation.

259 As a final experiment to substantiate the link between chitin binding,
260 intermolecular dimerization and polymerization, we performed limited ChELP2
261 digestion with thermolysin. Arguably, thermolysin will first of all target the
262 unstructured linker between the LysM domains rather than the highly structured LysM

263 domains themselves (Fig. 5C). Accordingly, after 5 min of thermolysin treatment a single
264 protein band that represents a single LysM domain could already be observed on
265 polyacrylamide gel, which increased in intensity at expense of the band that represents
266 the full-length LysM effector protein up to 1 h after thermolysin addition (Fig. 5D). While
267 a clear protein pellet was observed in untreated ChElp2 upon chitin addition followed
268 by centrifugation, no pellet formed for ChElp2 treated with thermolysin for 1 hr and
269 incubated with chitin (Fig. 5E). Thus, we conclude that the physical association of the
270 LysM domains is required to permit polymerization based on chitin-induced
271 intermolecular LysM dimerization of ChElp2.

272 To assess whether our conclusions for ChElp2 can be generalized and applies for
273 other dual-domain LysM effectors as well, the polymerization assay in the presence of
274 chitin was performed for *P. pastoris*-produced ChElp2, and for MoSlp1 and Vd2LysM as
275 well. Indeed, clear pellets were formed upon incubation of these proteins with chitin,
276 followed by centrifugation (Fig. 6). Collectively, our findings argue that dual-domain
277 LysM effectors undergo inter- rather than intramolecular dimerization upon chitin
278 binding, leading to polymerization of these LysM effectors.

279

280 **DISCUSSION**

281 We previously determined the mechanism for chitin binding for LysM effectors
282 composed of a single, or of three domains. However, many functionally characterized
283 LysM effectors are composed of two LysMs (Mentlak et al., 2012; Takahara et al., 2016;
284 Kombrink et al., 2017), and it remained unknown whether they are able to form a
285 composite chitin-binding groove through intrachain LysM dimerization to bind chitin
286 with ultrahigh affinity, such as the three-domain LysM effector Ecp6 (Sanchez-Vallet et
287 al., 2013; Sanchez-Vallet et al., 2015). Although our modelling studies based on three

288 software packages quite convincingly eliminated the possibility of intramolecular
289 dimerization, we set out to provide experimental evidence to support this notion and
290 pursued the determination of 3D-protein structures based on X-ray crystallography. We
291 screened the four dual-domain LysM effectors produced in *P. pastoris* as well as in *E. coli*
292 in different concentrations under 500 conditions in absence and presence of chitin in
293 different ratios, as well as with an additive screening in different buffers with a total of
294 nearly 200 conditions, but failed to develop protein crystals. Generally, if crystallization
295 of a protein fails, it can be attributed to many factors, ranging from insufficient purity
296 and homogeneity of the protein, to the fact that some proteins are simply naturally or
297 biologically unable to crystalize (Dessau and Modis, 2011; Wlodawer et al., 2017).
298 However, we then also considered the option that the lack of intramolecular LysM
299 dimerization would perhaps accommodate intermolecular LysM dimerization (Fig. 3A),
300 potentially leading to polymerization, which may lead to polymers of variable lengths
301 and, consequently, compromise protein homogeneity in solution leading to precipitation
302 rather than crystallization in turn. Thus, we decided to investigate the hypothesis that
303 exogenously added chitin induces intermolecular interaction between ChElp2
304 monomers (Fig. 3B), leading to polymer formation.

305 Through various lines of experimentation, we now provide solid evidence for the
306 absence of chitin-induced intramolecular dimerization, but rather the occurrence of
307 chitin-induced intermolecular dimerization of LysM domains of ChElp2 and other dual-
308 domain LysM effectors, leading to polymer formation *in vitro*. These experiments
309 include structural predictions, co-immunoprecipitation experiments, DLS measurements
310 of particle size distributions, centrifugation assays, mutant analyses and polymerization
311 assays with various substrates. The finding that Ecp6, in contrast to the dual-domain
312 LysM effectors, does not undergo chitin-induced polymerization is important, as it

313 demonstrates that the pellets are associated with intermolecular dimerization of LysM
314 effector molecules, a process that is not supposed to occur with Ecp6 that undergoes
315 intramolecular LysM dimerization (Sanchez-Vallet et al., 2013). Such protein pellet was
316 also not obtained for the mutant ChElp2$^{T49W-T120W}$ (Fig. 4C), indicating that chitin binding
317 is essential for ChElp2 polymerization. Yet, chitin binding in itself does not lead to
318 protein pellet formation, as limited protein digestion with thermolysin, that cleaves the
319 linker between the two LysMs and releases the individual LysM domains without
320 compromising their chitin-binding ability, did not lead to pellet formation (Fig. 5E).
321 Additionally, the polymerization assays in which ChElp2 was incubated with the chitin
322 dimer, trimer, tetramer, pentamer, hexamer and glucose (Fig. 5) revealed that it is not
323 the mere addition of chitin that leads to precipitation of protein pellets, as only those
324 molecules that have previously been shown to be bound by LysMs resulted in
325 polymerization, further implicating chitin binding as a requirement for the
326 polymerization to occur.

327 The apparent inability of dual-domain LysM effectors to undergo chitin-induced
328 intramolecular dimerization also implies that these LysM effectors cannot establish
329 ultrahigh affinity chitin-binding sites such as the one that was identified in *C. fulvum*
330 Ecp6 (Sánchez-Vallet et al., 2013). As this finding implies that the chitin binding
331 affinities of the dual-domain LysM effectors is markedly lower than that of Ecp6, it needs
332 to be acknowledged that these LysM effectors may not have the immediate capacity to
333 outcompete host immune receptors for chitin binding. Thus, we speculate that these
334 LysM effectors contribute to fungal virulence *in planta* through the formation of
335 polymeric complexes that have the propensity to precipitate in order to eliminate the
336 presence of freely available chitin oligomers at infection sites that may otherwise bind to
337 the host immune receptors. However, admittedly, experimental evidence for the

338 occurrence of such polymers *in planta* is currently lacking. Previously, we demonstrated
339 that the single LysM domain of Ecp6 that is not involved in the composite ultra-high
340 affinity binding groove, LysM2, can suppress chitin-triggered immunity, indicative of an
341 additional mechanism besides competitive chitin oligosaccharide sequestration
342 (Sánchez-Vallet et al., 2013). Importantly, as argued above, we demonstrated in the
343 current study that Ecp6 does not undergo chitin-induced polymerization. Rather, as
344 proposed previously, LysM2 of Ecp6, but potentially also the dual domain LysM effectors,
345 may perturb the immune receptor dimerization that is required for the activation of
346 immune signaling (Liu et al., 2012), compromising the activation of chitin-triggered
347 immunity in turn (Sánchez-Vallet et al., 2013). To this end, these effectors may
348 physically block host immune receptor dimerization by binding to chitin oligomers that
349 are attached to host immune receptor monomers. Thus, future efforts should be
350 dedicated to discriminate LysM effector precipitation upon polymerization from
351 receptor complex perturbation for the dual-domain LysM effectors when naturally
352 produced by fungi at infection sites during host colonization, momentarily a technically
353 very challenging undertaking.

354

355 **MATERIALS AND METHODS**

356 **Sequence alignment and three-dimensional protein structure prediction**

357 LysM domains of proteins were predicted by InterPro (Finn *et al.*, 2017) and the
358 alignment of amino acid sequences was performed by ClustalX2. Protein structures were
359 predicted with I-TASSER (Roy et al., 2010; Yang and Zhang, 2015), Phyre2 (Kelley *et al.*,
360 2015) and AlphaFold (Jumper et al., 2021) based on the composite chitin binding groove
361 composed of LysM1 and LysM3 of Ecp6. Structures were viewed by the PyMOL
362 molecular graphics system, version 2 (Schrodinger LLC, 2015).

363

364 **Heterologous protein production in *Pichia pastoris***

365 Protein sequences were analysed using SignalP4.0
366 (http://www.cbs.dtu.dk/services/SignalP; Petersen *et al.*, 2011) and the coding
367 sequences of mature proteins without signal peptide were amplified with primers listed
368 in Table S1, fused with an N-terminal 6×His-tag and cloned into expression vector pPIC9
369 (Thermo Fisher Scientific, California, USA). Correctness of the resulting constructs was
370 confirmed by DNA sequencing prior to introduction into *Pichia pastoris* strain GS115
371 (Thermo Fisher Scientific, California, USA). Fermentation was conducted in
372 approximately 3 L of culture in a bioreactor BioFlo120 (Eppendorf, Hamburg, Germany)
373 at 30°C for 5 days, including 3 days of methanol induction. Next, *P. pastoris* cells were
374 pelleted by centrifugation at 3800 g at 4°C for 50 min and the supernatant was
375 concentrated to 200 ml using a Vivaflow 200 Cross Flow Cassette (5000NWCO; Sartorius,
376 Göttingen, Germany) at 4°C for approximately 20 h. The concentrated supernatant was
377 purified using His60 Ni Superflow resin (TaKaRa, California, USA) on a BioLogic LP
378 system (Bio-Rad, California, USA). Purified protein was analysed by protein
379 polyacrylamide gel electrophoresis followed by staining with Coomassie Brilliant Blue
380 (CBB) and dialyzed against 5 L of 50 mM Tris, 150 mM NaCl to remove imidazole. Finally,
381 proteins were further concentrated using Amicon Ultra-15 Centrifugal Filter Units
382 (MERCK, Carrigtohill, Ireland) and stored at -20°C. Final concentrations of the four LysM
383 effectors are listed in Table S2.

384

385 **Heterologous protein production in *E. coli***

386 Coding sequences of mature proteins without signal peptide were amplified with
387 primers listed in Table S1 and cloned into expression vector pETSUMO (Thermo Fisher

388 Scientific, Massachusetts, USA). Correctness of the resulting constructs pETSUMO-
389 ChElp2 and pETSUMO-Vd2LysM were confirmed by DNA sequencing and introduced
390 into *E. coli* strains BL21 and Origami, respectively. FLAG-ChElp2 was amplified using
391 primers FLAG-ChElp2-F and ChElp2-R, cloned into pETSUMO and transformed into
392 BL21. All proteins were produced at 28°C with 0.2 mM IPTG. Cell culture was pelleted by
393 centrifugation at 4000 g for 40 min at 4°C, and the pellet was resuspended in 20 mL lysis
394 buffer (Table S3), shaken at 4°C for at least two hours and centrifuged at 10,000 g for 1 h.
395 The supernatant was collected and purified using His60 Ni Superflow resin (TaKaRa,
396 California, USA) on a BioLogic LP system (Bio-Rad, California, USA). The resulting
397 protein was dialyzed 3 L of 20 mM Tris, 150 mM NaCl, 5 % glycerol, pH 8.0 while 5 μL of
398 cleavage protein ULP1 was added into the dialysis membrane to cleave-off the 6×His-
399 SUMO tag. Next day, protein solution was collected and subjected to purification using
400 His60 Ni Superflow resin (TaKaRa, California, USA) to remove 6×His-SUMO tag from the
401 protein preparations. Eventually, *E. coli*-produced ChElp2 and Vd2LysM were buffer
402 exchanged in 20 mM Tris, 150 mM NaCl, 5% glycerol, pH 8.0 and concentrated to 5 and
403 4.3 mg/mL respectively.
404

405 **Glycoprotein staining assay**

406 1 μL of concentrated *P. pastoris*-produced LysM protein solution was tested using a
407 protein polyacrylamide gel followed by CBB and glycoprotein staining with the Pierce
408 Glycoprotein Staining Kit (Thermo Fisher Scientific, California, USA) according to the
409 manufacturer's instructions, including the addition of horseradish peroxidase and
410 soybean trypsin inhibitor as positive and negative control, respectively. *E. coli*-produced
411 ChElp2 and Vd2LysM were incubated with chitin hexamer overnight and subjected to
412 glycoprotein staining assay as described above.

413

414 **Deglycosylation assay**

415 Deglycosylation was performed PNGase F (MERCK, New Jersey, USA) and Protein
416 Deglycosyaltion Mix II (New England biolabs, Massachusetts, United State) according to
417 the manufacturer's instructions. Glycosylated fetuin was used as positive control. 5 μL of
418 MoSlp1, Vd2LysM and ChElp2 were treated with 10 μL of PNGase F at 37°C for 16 hours,
419 or with 10 μL of Protein Deglycosylation Mix II at 25°C for 30 min followed by
420 incubation at 37°C for 16 hours. Protein samples were collected at different time points
421 and analysed with protein polyacrylamide gel electrophoresis followed by CBB staining.

422

423 **Crystallization conditions**

424 Commercial kits PACT premier™ (Molecular dimensions, Sheffield, UK) and Salt^{RX},
425 Index^{TM}, Shotgun, PEG^{RX}, PEG/Ion screen (Hampton Research, California, USA) were
426 used for initial screening. 96-well protein crystallization plates were prepared using a
427 Crystal Phoenix robot (Art Robbins Instruments, California, USA). Chitohexaose
428 (Megazyme, Wicklow, Ireland) was added in molar ratios of 3:1 and 1:1. The additive
429 screening was conducted using the Additive Screen HR2-428 (Hampton Research,
430 California, USA) and Tacsimate pH 7.0 (Hampton Research, California, USA) according to
431 the manufacturer's instructions.

432

433 **Co-immunoprecipitation assay**

434 ChElp2 was produced in *E. coli* with either His-sumo-tag or FLAG-tag. 20 μM His-sumo-
435 ChElp2 and 40 μM FLAG-ChElp2 were incubated either individually or together in a total
436 volume of 600 μL in the absence and presence of 40 μM chitohexaose (Megazyme,
437 Wicklow, Ireland) at room temperature for 4-6 h. His-tagged ChElp2 was pulled-down

438 with Dynabeads™ His-Tag (Thermo Fisher Scientific, Massachusetts, USA) and the
439 subsequent western blot analyses were performed with anti-His (Sigma, Missouri, USA)
440 or anti-FLAG antibody (Sigma, Missouri, USA).
441
442 **Isothermal titration calorimetry**
443 Isothermal titration calorimetry (ITC) experiments were performed at 25°C using a
444 MicroCal PEAQ-ITC Automated (Malvern Panalytical, Worcestershire, UK) according to
445 the manufacturer's instructions. *E. coli*-produced LysM proteins were buffer exchanged in
446 50 mM Tris, 150 mM NaCl, 5% glycerol, pH 8.0. ChElp2 (20 μM) and ChElp2$^{T49W\text{-}T120W}$
447 (34 μM) were titrated with a first injection of 0.5 μL chitohexaose (Megazyme, Wicklow,
448 Ireland) with a concentration of 200 μM that was prepared in the same buffer with LysM
449 proteins, followed by another 20 injections of 2 μL. Data were analysed using Origin
450 (OriginLab, Northampton, MA, USA) and fitted to a one-binding-site model.
451
452 **Dynamic light scattering (DLS) measurements**
453 LysM proteins were dialyzed against 20 mM Tris, 150 mM NaCl, pH 8.0 overnight and
454 treated with 0.1% Triton X-100. Chitohexaose (Megazyme, Wicklow, Ireland) was
455 incubated with LysM proteins in protein:chitin molar ratios of 1:0, 1:3 and 1:6 overnight.
456 Next day, particle size distribution was measured with a Zetasizer Nano (Malvern
457 Panalytical, Worcestershire, UK). The data was visualized with Zetasizer software.
458
459 **Polymerization assays**
460 LysM effector proteins were adjusted to a concentration of 200 μM and 200 μL of each
461 protein was incubated with 200 μL of 2 mM diacetyl-chitobiose (Chi2), triacetyl-
462 chitobiose (Chi3), tetraacetyl-chitotetraose (Chi4), pentaacetyl-chitopentaose (Chi5),

463 hexaacetyl-chitohexaose (Chi6) (Megazyme, Wicklow, Ireland), glucose (Merck,
464 Darmstadt, Germany), or 200 μL water as control, at room temperature overnight. The
465 next day, 2 μL of 0.2% methylene blue (Sigma-Aldrich, Missouri, USA) was added and
466 incubated for 30 min after which protein solutions were centrifuged at 20,000 g for 15
467 min. Photos were taken with a ChemiDoc XRS+ system (Bio-Rad, California, USA) with
468 custom setting for RFP or with a ChemiDoc system (Bio-Rad, California, USA) with the
469 setting of Coomassie Blue with white tray (Bio-rad, California, USA).

470 For limited digestion assay with thermolysin, 10 μL of ChElp2 (200 μM) was
471 incubated with 5 μL of 1 mg/ml thermolysin at 55°C for 3 hours. Protein samples were
472 collected at different time points and analysed with a protein polyacrylamide gel.
473 Subsequently, ChElp2 was digested with thermolysin for 1 h, deactivated the protease
474 according to manufacturer's instructions and incubated with chitin hexamer overnight.
475 The next day, 2 μL of 0.2% methylene blue (Sigma-Aldrich, Missouri, USA) was added
476 and incubated for 30 min. After centrifugation at 20,000 g for 15 min, photos were taken
477 with a ChemiDoc system (Bio-Rad, California, USA) with the setting of Coomassie Blue
478 with white tray (Bio-rad, California, USA).

479

480 **ACKNOWLEDGEMENTS**

481 H.T. acknowledges receipt of a PhD fellowship from the China Scholarship Council (CSC)
482 and G.L.F acknowledges receipt of a PhD fellowship from the Coordination for the
483 Improvement of Higher Education Personnel (CAPES) from the federal government of
484 Brazil. B.P.H.J.T acknowledges funding by the Alexander von Humboldt Foundation in
485 the framework of an Alexander von Humboldt Professorship endowed by the German
486 Federal Ministry of Education and Research, and is furthermore supported by the
487 Deutsche Forschungsgemeinschaft (DFG, German Research Foundation) under

Germany´s Excellence Strategy – EXC 2048/1 – Project ID: 390686111. The authors declare no conflict of interest exists.

AUTHOR CONTRIBUTIONS

HT, JRM, BPHJT conceived the study; HT, JRM, BPHJT designed experiments; HT, GLF and AK performed experiments; HT, JRM, BPHJT analyzed data and wrote the manuscript; JRM and BPHJT supervised the project; all authors discussed the results and contributed to the final manuscript.

CONFLICT OF INTEREST

The authors declare no conflict of interest exists.

499 **REFERENCES**

500 **Altenbach D, Robatzek S** (2007) Pattern recognition receptors: from the cell surface to
501 intracellular dynamics. Mol Plant-Microbe Interact **20**: 1031–1039

502 **Baker HM, Day CL, Norris GE, Baker EN** (1994) Enzymatic deglycosylation as a tool for
503 crystallization of mammalian binding proteins. Acta Crystallogr D Biol Crystallogr
504 **50**: 380–384

505 **Bateman A, Bycroft M** (2000) The structure of a LysM domain from E. coli membrane-
506 bound lytic murein transglycosylase D (MltD). J Mol Biol **299**: 1113–1119

507 **Boller T, Felix G** (2009) A renaissance of elicitors: perception of microbe-associated
508 molecular patterns and danger signals by pattern-recognition receptors. Annu Rev
509 Plant Biol **60**: 379–406

510 **Bolton MD, Van Esse HP, Vossen JH, De Jonge R, Stergiopoulos I, Stulemeijer IJE,**
511 **Van Den Berg GCM, Borrás-Hidalgo O, Dekker HL, De Koster CG, et al** (2008)
512 The novel Cladosporium fulvum lysin motif effector Ecp6 is a virulence factor with
513 orthologues in other fungal species. Mol Microbiol **69**: 119–136

514 **Cao Y, Liang Y, Tanaka K, Nguyen CT, Jedrzejczak RP, Joachimiak A, Stacey G** (2014)
515 The kinase LYK5 is a major chitin receptor in Arabidopsis and forms a chitin-
516 induced complex with related kinase CERK1. Elife **3**: e03766

517 **Cen K, Li B, Lu Y, Zhang S, Wang C** (2017) Divergent LysM effectors contribute to the
518 virulence of Beauveria bassiana by evasion of insect immune defenses. PLOS Pathog
519 **13**: e1006604

520 **Chen XL, Shi T, Yang J, Shi W, Gao X, Chen D, Xu X, Xu JR, Talbot NJ, Peng YL** (2014)
521 N-Glycosylation of effector proteins by an α-1,3-Mannosyltransferase is required
522 for the rice blast fungus to evade host innate immunity. Plant Cell **26**: 1360–1376

523 **Davis SJ, Puklavec MJ, Ashford DA, Harlos K, Jones EY, Stuart DI, Williams AF** (1993)
524 Expression of soluble recombinant glycoproteins with predefined glycosylation:
525 application to the crystallization of the T-cell glycoprotein CD2. Protein Eng **6**: 229–
526 232

527 **Dessau MA, Modis Y** (2011) Protein crystallization for X-ray crystallography. J Vis Exp
528 **16**: 2285

529 **Dolfors F, Holmquist L, Dixelius C, Tzelepis G** (2019) A LysM effector protein from the
530 basidiomycete Rhizoctonia solani contributes to virulence through suppression of
531 chitin-triggered immunity. Mol Genet Genomics **294**: 1211–1218

532 **Felix G, Regenass M, Boller T** (1993) Specific perception of subnanomolar
533 concentrations of chitin fragments by tomato cells: Induction of extracellular
534 alkalinization, changes in protein phosphorylation, and establishment of a
535 refractory state. Plant J **4**: 307–316

536 **Finn RD, Attwood TK, Babbitt PC, Bateman A, Bork P, Bridge AJ, Chang HY,**
537 **Dosztanyi Z, El-Gebali S, Fraser M, et al** (2017) InterPro in 2017-beyond protein
538 family and domain annotations. Nucleic Acids Res **45**: D190–D199

539 **Free SJ** (2013) Fungal cell wall organization and biosynthesis. Adv Genet **81**: 33–82

540 **Haltiwanger RS, Lowe JB** (2004) Role of glycosylation in development. Annu Rev
541 Biochem **73**: 491–537

542 **Jones JDG, Dangl JL** (2006) The plant immune system. Nature **444**: 323–329

543 **de Jonge R, van Esse P, Kombrink A, Shinya T, Desaki Y, Bours R, van der Krol S,**
544 **Shibuya N, Joosten MHAJ, Thomma BPHJ** (2010) Conserved fungal LysM effector
545 Ecp6 prevents chitin-triggered immunity in plants. Science (80-) **329**: 953–955

546 **Jumper J, Evans R, Pritzel A, Green T, Figurnov M, Ronneberger O,**
547 **Tunyasuvunakool K, Bates R, Žídek A, Potapenko A, et al** (2021) Highly accurate
548 protein structure prediction with AlphaFold. Nature **596**: 583–589

549 **Kelley LA, Mezulis S, Yates CM, Wass MN, Sternberg MJE** (2015) The Phyre2 web
550 portal for protein modeling, prediction and analysis. Nat Protoc **10**: 845–858

551 **Kombrink A, Rovenich H, Shi-Kunne X, Rojas-Padilla E, van den Berg GCM,**
552 **Domazakis E, de Jonge R, Valkenburg DJ, Sánchez-Vallet A, Seidl MF, et al**
553 (2017) Verticillium dahliae LysM effectors differentially contribute to virulence on
554 plant hosts. Mol Plant Pathol **18**: 596–608

555 **Kombrink A, Thomma BPHJ** (2013) LysM effectors: secreted proteins supporting
556 fungal life. PLOS Pathog **9**: e1003769

557 **Lenardon MD, Munro CA, Gow NA** (2010) Chitin synthesis and fungal pathogenesis.
558 Curr Opin Microbiol **13**: 416–423

559 **Liu T, Liu Z, Song C, Hu Y, Han Z, She J, Fan F, Wang J, Jin C, Chang J, Zhou JM, Chai J.**
560 (2012) Chitin-induced dimerization activates a plant immune receptor. Science **336**:
561 1160-1164

562 **Marshall R, Kombrink A, Motteram J, Loza-Reyes E, Lucas J, Hammond-Kosack KE,**
563 **Thomma BPHJ, Rudd JJ** (2011) Analysis of two in planta expressed LysM effector
564 homologs from the fungus *Mycosphaerella graminicola* reveals novel functional
565 properties and varying contributions to virulence on wheat. Plant Physiol **156**:
566 756–769

567 **Mentlak TA, Kombrink A, Shinya T, Ryder LS, Otomo I, Saitoh H, Terauchi R,**
568 **Nishizawa Y, Shibuya N, Thomma BPHJ, et al** (2012) Effector-mediated
569 suppression of chitin-triggered immunity by *Magnaporthe oryzae* is necessary for
570 rice blast disease. Plant Cell **24**: 322–335

571 **Miya A, Albert P, Shinya T, Desaki Y, Ichimura K, Shirasu K, Narusaka Y, Kawakami**
572 **N, Kaku H, Shibuya N** (2007) CERK1, a LysM receptor kinase, is essential for chitin
573 elicitor signaling in Arabidopsis. Proc Natl Acad Sci U S A **104**: 19613–19618

574 **Moremen KW, Tiemeyer M, Nairn A V** (2012) Vertebrate protein glycosylation:
575 diversity, synthesis and function. Nat Rev Mol Cell Biol **13**: 448–462

576 **Nagashima Y, von Schaewen A, Koiwa H** (2018) Function of N-glycosylation in plants.
577 Plant Sci **274**: 70–79

578 **Petersen TN, Brunak S, von Heijne G, Nielsen H** (2011) SignalP 4.0: discriminating
579 signal peptides from transmembrane regions. Nat Methods **8**: 785–786

580 **Petutschnig EK, Jones AME, Serazetdinova L, Lipka U, Lipka V** (2010) The Lysin
581 Motif Receptor-like Kinase (LysM-RLK) CERK1 is a major chitin-binding protein in
582 Arabidopsis thaliana and subject to chitin-induced phosphorylation. J Biol Chem
583 **285**: 28902–28911

584 **Proteau A, Shi R, Cygler M** (2010) Application of dynamic light scattering in protein
585 crystallization. Curr Protoc Protein Sci **Chapter 17**: Unit 17 10

586 **Rovenich H, Boshoven JC, Thomma BPHJ** (2014) Filamentous pathogen effector
587 functions: Of pathogens, hosts and microbiomes. Curr Opin Plant Biol **20**: 96–103

588 **Rovenich H, Zuccaro A, Thomma BP** (2016) Convergent evolution of filamentous

589 microbes towards evasion of glycan-triggered immunity. New Phytol **212**: 896–901

590 **Roy A, Kucukural A, Zhang Y** (2010) I-TASSER: a unified platform for automated
591 protein structure and function prediction. Nat Protoc **5**: 725–738

592 **Sanchez-Vallet A, Mesters JR, Thomma BPHJ** (2015) The battle for chitin recognition
593 in plant-microbe interactions. FEMS Microbiol Rev **39**: 171–183

594 **Sanchez-Vallet A, Saleem-Batcha R, Kombrink A, Hansen G, Valkenburg DJ,**
595 **Thomma BPHJ, Mesters JR** (2013) Fungal effector Ecp6 outcompetes host immune
596 receptor for chitin binding through intrachain LysM dimerization. Elife **2**: e00790

597 **Sánchez-Vallet A, Tian H, Rodriguez-Moreno L, Valkenburg D-J, Saleem-Batcha R,**
598 **Wawra S, Kombrink A, Verhage L, de Jonge R, van Esse HP, et al** (2020) A
599 secreted LysM effector protects fungal hyphae through chitin-dependent
600 homodimer polymerization. PLoS Pathog **16**: 1–21

601 **Schrodinger LLC** (2015) The JyMOL Molecular Graphics Development Component,
602 Version 1.8.

603 **Takahara H, Hacquard S, Kombrink A, Hughes HB, Halder V, Robin GP, Hiruma K,**
604 **Neumann U, Shinya T, Kombrink E, et al** (2016) *Colletotrichum higginsianum*
605 extracellular LysM proteins play dual roles in appressorial function and
606 suppression of chitin-triggered plant immunity. New Phytol **211**: 1323–1337

607 **Tang J, Sun Y, Han Z, Shi W** (2019) An illustration of optimal selected glycosidase for N-
608 glycoproteins deglycosylation and crystallization. Int J Biol Macromol **122**: 265–271

609 **Tian H, MacKenzie CI, Rodriguez-Moreno L, van den Berg GCM, Chen H, Rudd JJ,**
610 **Mesters JR, Thomma BPHJ** (2021) Three LysM effectors of *Zymoseptoria tritici*
611 collectively disarm chitin-triggered plant immunity. Mol Plant Pathol 1–11

612 **Wlodawer A, Dauter Z, Jaskolski M** (2017) Protein crystallography: methods and
613 protocols. Humana Press **1607**: 672

614 **Xu C, Ng DT** (2015) Glycosylation-directed quality control of protein folding. Nat Rev
615 Mol Cell Biol **16**: 742–752

616 **Yang J, Zhang Y** (2015) I-TASSER server: new development for protein structure and
617 function predictions. Nucleic Acids Res **43**: W174-81

618 **Zeng T, Rodriguez-Moreno L, Mansurkhodzaev A, Wang P, van den Berg W,**

619 **Gasciolli V, Cottaz S, Fort S, Thomma B, Bono JJ, et al** (2020) A lysin motif
620 effector subverts chitin-triggered immunity to facilitate arbuscular mycorrhizal
621 symbiosis. New Phytol **225**: 448–460

622 **Zhang X-C, Wu X, Findley S, Wan J, Libault M, Nguyen HT, Cannon SB, Stacey G**
623 (2007) Molecular Evolution of Lysin Motif-Type Receptor-Like Kinases in Plants.
624 Plant Physiol **144**: 623–636

625 **Zipfel C** (2008) Pattern-recognition receptors in plant innate immunity. Curr Opin
626 Immunol **20**: 10–16

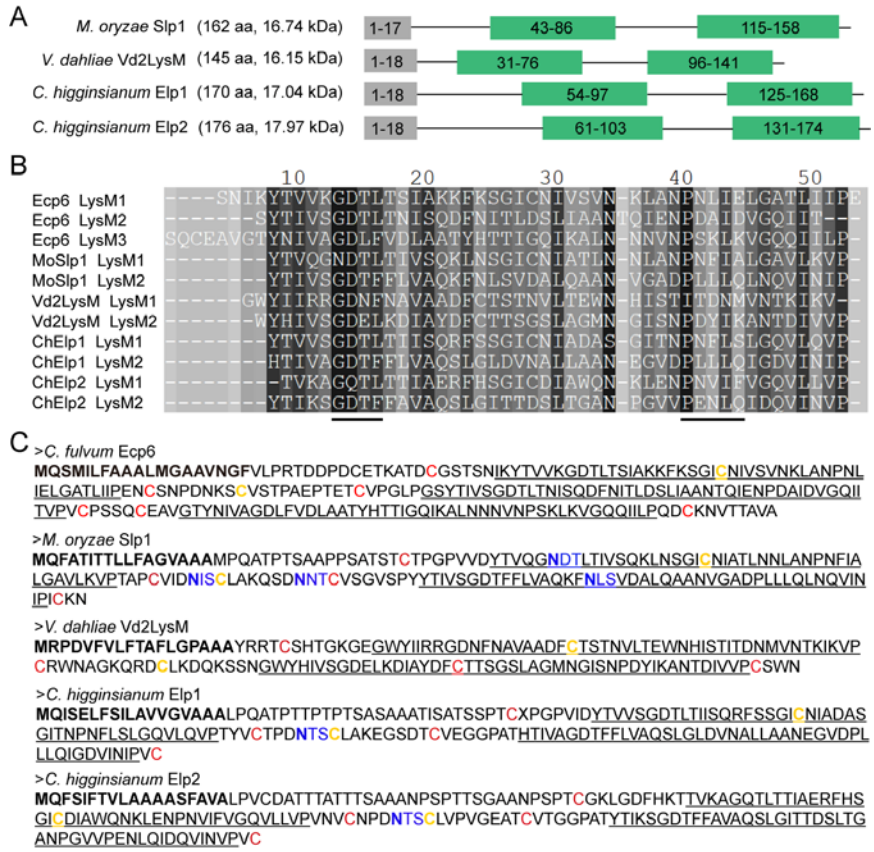

Figure 1. Conservation of chitin binding sites and of disulfide bond formation among Ecp6 and the four dual-domain LysM effectors. (A) Schematic representation of the four fungal dual-domain LysM effectors: *Magnaporthe oryzae* MoSlp1, *Verticillium dahliae* Vd2LysM, and *Colletotrichum higginsianum* ChElp1 and ChElp2. Signal peptides (grey boxes) were predicted with SignalP 4.0 (http://www.cbs.dtu.dk/services/SignalP-4.0/) and LysM domains (green boxes) with InterPro (https://www.ebi.ac.uk/interpro/). The amino acid numbers that compose the motif are indicated in the boxes. (B) Amino acid sequence alignment of the LysM domains of MoSlp1, Vd2LysM, ChElp1 and ChElp2 in comparison with those of Ecp6. The black lines indicate chitin-binding sites. (C) Amino acid sequences of Ecp6, MoSlp1, Vd2LysM, ChElp1 and ChElp2 with signal peptides in bold, LysM domains underlined and the putative *N*-glycosylation sites highlighted in blue with the asparagines that may be N-glycosylated in blue bold font. Cysteine residues involved in disulfide bond formation are indicated red and green with those involved in disulfide bonds within individual LysM domains in red, and those involved in the bond between LysM1 and the linkers between the two LysM domains in yellow.

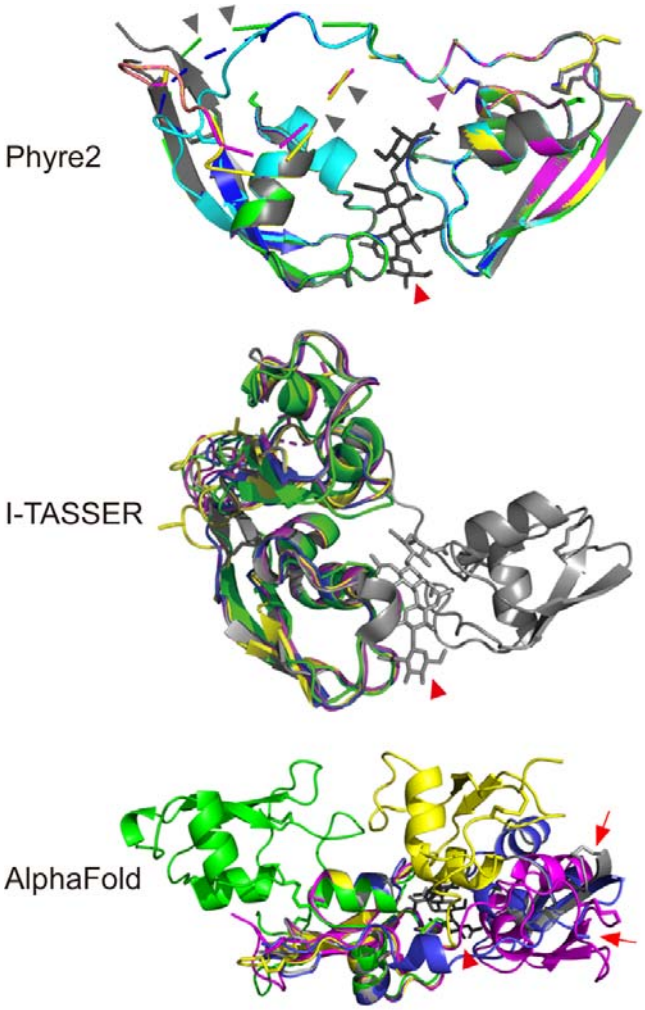

642

643 **Figure 2. *In-silico* prediction of the three-dimensional structures of MoSlp1, Vd2LysM,**
644 **ChElp1 and ChElp2.** The prediction was conducted based on the composite chitin binding
645 groove composed of LysM1 and LysM3 of Ecp6 (Sánchez-Vallet et al., 2013) with Ecp6 in grey,
646 MoSlp1 in yellow, Vd2LysM in green, ChElp1 in blue, and ChElp2 in purple. Furthermore, for the
647 Phyre2 prediction, ChElp2 carrying an artificial insertion of 5-amino acid (GGSGG) in the linker
648 between the two LysMs is indicated in cyan. Red arrowheads indicate a chitin tetramer in the
649 Ecp6 LysM1-LysM3 binding groove. Purple and grey arrowheads indicate predicted disulphide
650 bonds for MoSlp1, ChElp1 and ChElp2 and disrupted linkers for the four dual-domain LysM
651 effectors, respectively. The red arrows indicate the questionable offset position of C99 in the
652 ChElp1 AlphaFold predicted structure (blue) and of C139 in the crystal structure of Ecp6 (grey).

All structures were visualized using the PyMOL molecular graphics system (Schrodinger LLC, 2015).

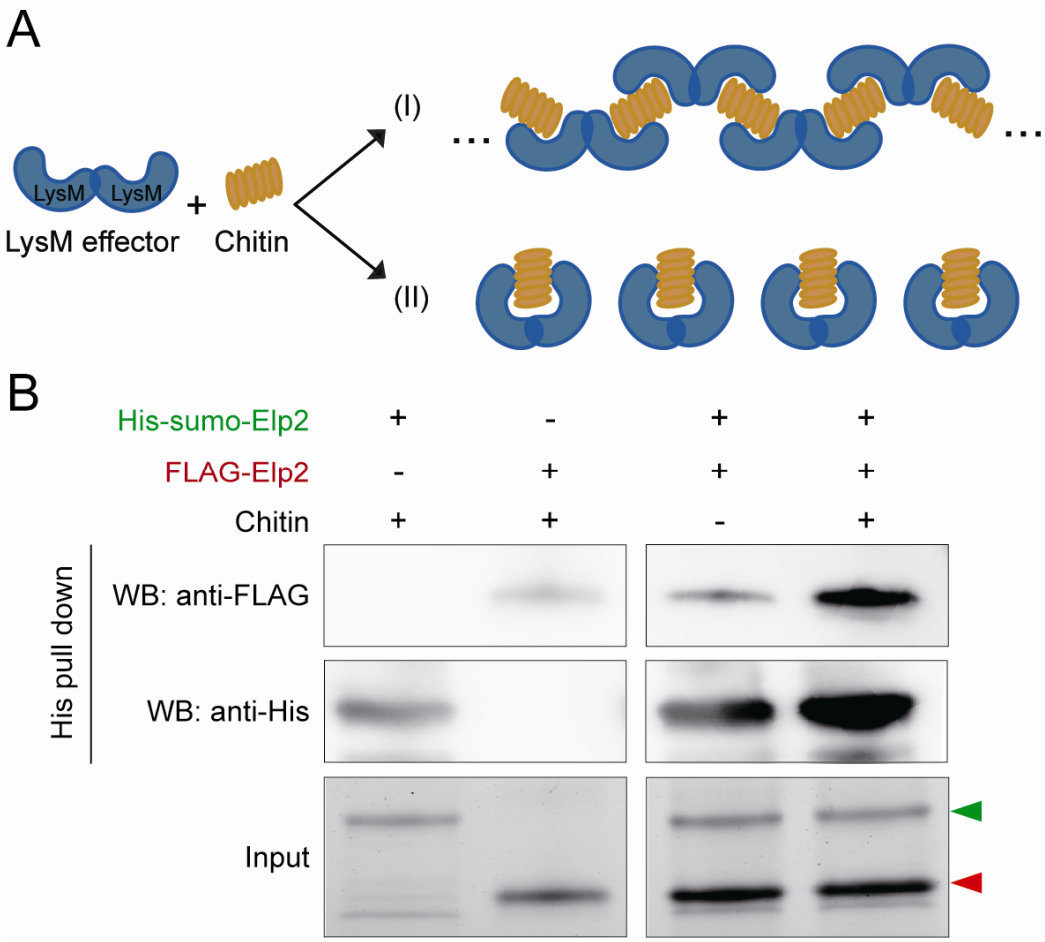

Figure 3. ChElp2 binds chitin via intermolecular LysM dimerization. (A) Two hypotheses for chitin binding by dual-domain LysM effectors that may bind chitin through: (I) intermolecular dimerization in which LysM effectors may undergo ligand-induced polymerization, or through: (II) intramolecular dimerization that should not lead to polymerization. (B) *Escherichia coli*-produced His-sumo-ChElp2 and FLAG-ChElp2 were incubated either individually in the presence of chitin or together in the absence and presence of chitin for 4-6 hours. His-sumo-ChElp2 was pulled-down by anti-His magnetic beads and the subsequent western blot analysis was performed with either anti-FLAG or anti-His antibody. Green and red arrow heads indicate the molecular sizes of His-sumo-Elp2 and FLAG-Elp2 on protein polyacrylamide gel, respectively.

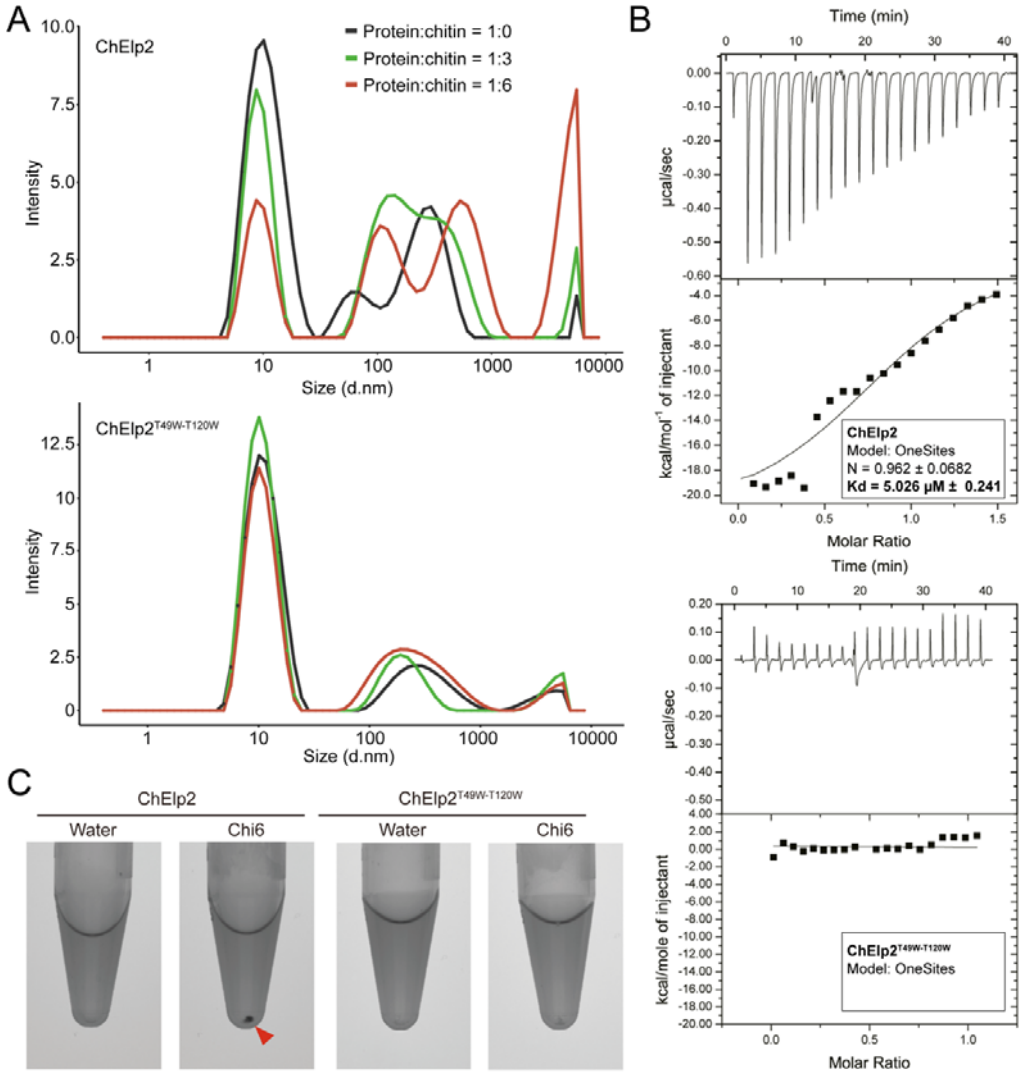

Figure 4. ChElp2 undergoes chitin-induced polymerization. (A) ChElp2 particle size distribution in protein solution with diameter values in nanometers (d.nm) measured by dynamic light scattering (DLS). (B) Raw data and integrated heat measurements from isothermal titration calorimetry of chitohexose binding to wild-type ChElp2 and the mutant ChElp2$^{T49W-T120W}$ in which the threonine within each of the LysM domains that is critical for chitin binding (LysM1, T49; LysM2, T120) was replaced by tryptophan. Lines in the lower panel represent best-fit curves for a one binding-site model. (C) ChElp2 and ChElp2$^{T49W-T120W}$ were incubated with chitin hexamer or water as control. After overnight incubation, methylene blue was added and protein solutions were centrifuged, resulting in protein pellets (red arrowheads) as a consequence of polymerization.

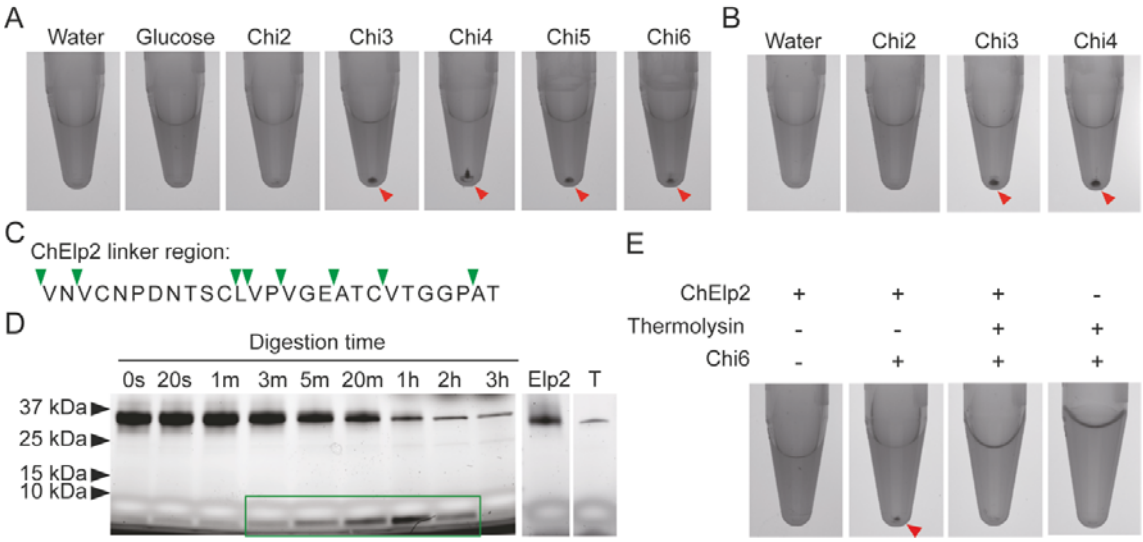

Figure 5. Chitin-binding and the physical association of the two LysM domains are required for ChElp2 polymerization. (A) 100 µM ChElp2 was incubated with 1 mM diacetyl-chitobiose (Chi2), triacetyl-chitotriose (Chi3), tetraacetyl-chitotetraose (Chi4), pentaacetyl-chitopentaose (Chi5), hexaacetyl-chitohexaose (Chi6) or glucose in a total volume of 400 µL. After overnight incubation, methylene blue was added and protein solutions were centrifuged, resulting in protein pellets that are indicated by red arrowheads. (B) 100 µM ChElp2 was incubated with Chi2 (3 mM), Chi3 (2 mM) and Chi4 (1.5 mM) in a total volume of 400 µL such that the final amount of GlcNAc units is the same for all incubations. After overnight incubation, methylene blue was added and protein solutions were centrifuged, resulting in protein pellets that are indicated by red arrowheads. (C) Amino acid sequence of the ChElp2 linker between the two LysMs with putative thermolysin cleavage sites indicated by green arrowheads. (D) *P. pastoris*-produced ChElp2 was incubated with thermolysin (T) for 3 hours, protein samples were collected at different time points and analysed on protein polyacrylamide gel. (E) *P. pastoris*-produced ChElp2 incubated with or without thermolysin for 1 hour, followed by overnight incubation with chitin hexamer or water. Methylene blue was added and the protein solutions were centrifuged, resulting in protein pellets that are indicated by red arrowheads.

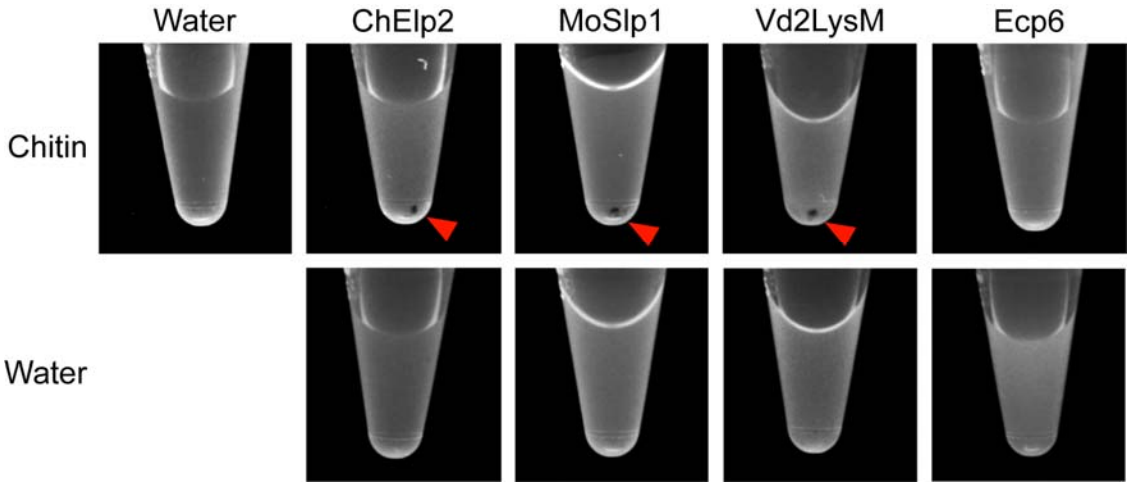

693

694 **Figure 6. Chitin-induced polymerization of dual-domain LysM effectors.** (A) The LysM
695 effector proteins ChElp2, MoSlp1 and Vd2LysM, together with Ecp6 as negative control, were
696 incubated with chitin hexamer or water. After overnight incubation, methylene blue was added
697 and protein solutions were centrifuged, resulting in protein pellets that are indicated by red
698 arrowheads.